Colloid Polym Sci (2017) 295:715–724
DOI 10.1007/s00396-017-4055-3

SHORT COMMUNICATION

Sonolytic doping of poly(1-naphthylamine) with luminol: influence on spectral, morphological and fluorescent characteristics

Sapana Jadoun[1] · **Vivek Sharma**[2] · **S. M. Ashraf**[1] · **Ufana Riaz**[1]

Received: 18 January 2017 / Revised: 18 February 2017 / Accepted: 21 February 2017 / Published online: 6 March 2017

Abstract Doping is one of the most facile techniques adopted to improve the optoelectronic properties of conducting polymers. The present preliminary work reports, for the first time, chemical doping of poly(1-napthylamine) (PNA) with (5-amino-2,3-dihydro-1,4-phthalazine-dione) widely known as luminol, to study its influence on the spectral, morphological, and optical properties of PNA. PNA was doped with luminol in acidic, basic, and neutral media. The neutral polymer and its doped forms were characterized using FTIR, UV-visible, XRD, and TEM analyses. FTIR studies confirmed doping of PNA by luminol, while UV-visible and fluorescence studies revealed the changes in the electronic structure of PNA upon doing. Confocal microscopy revealed intense red emission confirming that the polymers could be used for near infrared fluorescence imaging.

Keywords Luminol · Poly(1-naphthylamine) · Near infrared fluorescence · Doping · Confocal imaging

Introduction

Conjugated polymeric nanoparticles such as polyacetylenes (PAcs) [1], polyanilines (PANIs) [2], polypyrroles [3], polyfluorenes (PFs) [4], poly(arylenevinylenes) (PArVs) [5], poly(phenylene ethylene vinylenes) (PEVs) [6], polythiophenes (PThs) [7], poly(1-naphthylamine) (PNA) [8], and poly(carbazole) (PCz) [9] are extensively explored due to their unique optoelectronic and thermal properties as well as good environmental stability [10, 11]. Among the several aniline derivatives, poly(1-naphthylamine) (PNA) has been widely reported due to its unique electrochemical characteristics [8, 12–14]. Luminol (5-amino-2,3-dihydro-1,4-phthalazine-dione) is a well-known chemiluminescent material which is widely used in forensic detection of blood stains [15–20]. The chemiluminescence intensity in luminol is enhanced due to the electron donating nature of amino group which exhibits positive mesomeric effect. Proesher and Moody [21] investigated the chemical structure as well as the nature of reactivity of luminol and predicted the keto-enolic tautomerization of luminol in basic solutions and the fully protonated form in acidic solutions.

Until now, no literature has been reported based on the doping of PNA with luminol in basic, acidic, and neutral media via sonolytic doping. Ultrasound irradiation is widely used in heterogeneous reactions dealing with organic phase insoluble solutions [22, 23]. Compared with traditional methods, this method can be used for carrying out reactions in milder state and in a short span of time [23, 24]. Therefore, to understand the role of luminol as a dopant, the present preliminary study reports the ultrasound-assisted synthesis of PNA and its doping with luminol under acidic, basic, and neutral solutions. The synthesized polymer and its doped forms were investigated for their spectral, morphological, and fluorescent characteristics. It was observed that doping of PNA luminol had a profound influence on its spectral and morphological properties which could be utilized to design near infrared emitting polymers.

S. M. Ashraf is now retired

✉ Ufana Riaz
ufana2002@yahoo.co.in

[1] Materials Research Laboratory, Department of Chemistry, Jamia Millia Islamia, New Delhi 110025, India

[2] Department of Chemistry, Indian Institute of Technology Roorkee, Roorkee, Uttarakhand 247667, India

Table 1 CHNS, intrinsic viscosity, and molar mass of PNA and doped PNA

Sample	N%		C %		H %		Empirical formula	Intrinsic viscosity (η)	Molar mass (M_v)
	Found	Calculated	Found	Calculated	Found	Calculated			
PNA	7.07	19.31	60.78	73.73	4.30	4.13	$C_{10.03}H_{8.51}N$	0.49	21,528
PNA-luminol-basic	7.97	14.01	71.42	74.73	4.21	4.11	$C_{10.45}H_{7.38}N$	0.59	38,278
PNA-luminol-acidic	6.92	7.73	71.45	74.25	4.41	4.09	$C_{12\cdot04}H_{8.93}N$	0.61	42,419
PNA-luminol-neutral	6.55	13.82	70.79	74.14	4.39	4.63	$C_{12.61}H_{9.381}N$	0.55	30,814

Synthesis and characterization

Materials

1-Naphthylamine (NA), luminol (Lu), 1-methyl-2-pyrollidone (NMP), and ferric chloride were purchased from Sigma-Aldrich, USA, and were used without further purification. Sodium hydroxide (NaOH), hydrogen peroxide (H_2O_2), and tetrahydrofuran (THF) was procured from Merck India and were also used as such.

Ultrasound-assisted synthesis of poly(1-naphthylamine)

Monomer 1-naphthylamine (4 g, 0.028 mol) (monomer) was added to an Erlenmeyer flask (100 ml) containing deionized water (30 ml). The solution was stirred at room temperature for 30 min. A solution of ferric chloride ((4.53 g, 0.027 mol) (oxidant) dissolved in 20 ml deionized water) was then added to above reaction mixture (keeping the mole ratio of monomer/oxidant as 1:1) and sonicated for 5 h at 25 °C, using ultrasonic frequency of 150 kHz and ultrasonic power of 300 W. The color of solution changed from purple to black indicating polymerization of 1-naphthylamine [8]. After sonication, the reaction flask was kept overnight in a deep freezer at −10 °C. The synthesized polymer was then centrifuged and washed several times with distilled water and ethanol. The removal of excess of ferric chloride was ensured by testing the filtrate with potassium ferrocyanide. The obtained polymer was then dried in a vacuum oven at 70 °C for 72 h. The polymer was designated as PNA and the % yield was calculated to be 93.23%.

Preparation of acidic, basic, and neutral luminol solutions and doping with PNA

For the preparation of basic solution of luminol, NaOH (0.99 g, 0.024 mol) was added to a conical flask (500 ml) containing deionized water (250 ml). The solution was stirred on a magnetic stirrer for 4 h at 25 °C. Luminol (1.77 g, 0.01 mol) was added to above solution and stirred for another 3 h at the same temperature. The preparation of acidic solution of luminol was carried out by adding H_2O_2 (0.5683 ml, 0.1 mol) to deionized water (100 ml) in a 500-ml flask stirred on a magnetic stirrer for 4 h at 25 °C. Luminol (1.77 g, 0.01 mol) was added to the above solution and stirred for another 3 h at the same temperature. Similarly, for the preparation of neutral solution of luminol (1.77 g, 0.01 mol), luminol was added to 100 ml deionized water and stirred under the same conditions.

Doping of PNA by the above solutions was carried out by taking PNA (500 mg) in a 250-ml flask and 100 ml of each of the acidic, basic, and neutral luminol solutions. The solutions were sonicated for 12 h at 25 °C in an ultrasonicator, at ultrasonic frequency of 150 kHz and ultrasonic power of 300 W. All the three flasks were then kept undisturbed in deep freezer overnight at 10 °C. After 24 h, the doped polymer solutions were centrifuged washed several times with distilled water. The obtained doped polymers were then dried in a vacuum oven for 72 h at 40 °C to ensure complete removal of water and other impurities. The doped forms of PNA were designated as PNA-luminol-basic, PNA-luminol-acidic, and PNA-luminol-neutral, respectively.

Characterization

CHNS analysis of homopolymer and doped polymers was carried out using a Perkin-Elmer Series II 2400 CHNSO Analyzer. Viscosity average molecular weight was determined by taking 0.4 wt% solution of the polymer in NMP using Ubbelhode viscometer at room temperature, and the intrinsic viscosity was determined using the Mark-Houwink equation: $[\eta] = 2.0 \times 10^{-2} M_v^{0.3176}$, M_v is viscosity average molecular weight, and K and a are Mark-Houwink constants [25].

FT-IR spectra of polymers and doped polymers were taken on FT-IR spectrophotometer model Shimadzu IRA Affinity-1 in the form of KBr pellets. The integrated absorption coefficient, $\int a d\bar{\nu}$, was determined using the IRA Affinity-1 software through Gaussian-Lorentzian curve fittings. UV-visible spectra were recorded in solution state using THF as solvent on UV-visible spectrophotometer model Shimadzu UV-1800. The molar extinction coefficient and oscillator strength were calculated as reported in our earlier studies [26, 27]. X-ray

Table 2 FTIR spectra of PNA and luminol doped PNAs

Sample	Functional group	Peak position/absorption intensity (cm^{-1})	Benzenoid/ quinonoid ratio
PNA	NH-stretching	3414/0.80	1.07
	Imine stretching	1639/0.45	
	C-C stretching (quinonoid)	1523/0.28	
	C-C stretching (benzenoid)	1492/0.30	
	CN stretching	1253/0.22	
	C–H stretching (bending) of substituted benzene (1–4 coupling)	765/0.20	
PNA-luminol-basic	NH-stretching	3415/1.7	1.0
	C = O stretching	1713/0.68	
	Imine stretching	1620/0.85	
	C-C stretching (quinonoid)	1535/0.60	
	C-C stretching (benzenoid)	1490/0.60	
	CN stretching	1254/0.43	
	C–H stretching (bending) of substituted benzene (1–4 coupling)	771/0.14	
PNA-luminol-acidic	NH-stretching	3421/1.18	0.34
	C = O stretching	1690/0.39	
	Imine stretching	1639/0.56	
	C-C stretching (quinonoid)	1513/0.93	
	C-C stretching (benzenoid)	1491/0.32	
	CN stretching	1252/0.25	
	C–H stretching (bending) of substituted benzene (1–4 coupling)	769/0.138	
PNA-luminol-neutral	NH-stretching	3421/1.52	0.98
	Imine stretching	1630/0.80	
	C-C stretching (quinonoid)	1510/0.55	
	C-C stretching (benzenoid)	1491/0.54	
	CN stretching	1251/0.45	
	C–H stretching (bending) of substituted benzene (1–4 coupling)	770/0.32	

diffraction patterns of the polymer and its doped forms were recorded on Philips PW 3710 powder diffractometer (Nickel filtered Cu-Kα radiation). Optical microscopic images were taken using Banbros polarizing microscope, model Banbros, India. Images were taken at a magnification of ×1000. Transmission electron micrographs (TEM) were taken on Morgagni 268-D TEM, FEI, USA, operated at an accelerated voltage of 120 kV. The samples were prepared by placing a dispersion of the sample on carbon-coated copper grid, subsequently drying in air before transferring it to the microscope, operated at an accelerated voltage of 120 kV. Fluorescence spectroscopy was performed by preparing solutions of the polymer and its doped forms in THF, and the spectra were recorded on fluorescence spectrofluorometer model Fluorolog-3-11 (Horiba). The quantum yield (ϕ) was calculated as per method reported in our earlier studies [26, 27]. Fluorescence images were taken with a ×100 objective at room temperature using a Laser Confocal Microscope with Fluorescence Correlation Spectroscopy (FCS) - Olympus FluoView™ FV1000 equipped with He-Ne laser and oil immersion objective λ_{max} for laser excitation was 410 nm.

Results and discussion

Confirmation of doping by CHNS, viscosity, and FTIR studies

To calculate intrinsic viscosity of synthesized polymers, dilute solution viscometric technique was adopted. A 0.4 wt% polymer solution was taken in NMP, and by determining the intrinsic viscosity, molecular weight was calculated using Mark-Houwink equation: $[\eta] = KM_v^a$, where η is the intrinsic viscosity, $[\eta] = 2.0 \times 10^{-2}\ M_v^{0.3176}$, M_v is molecular weight, K and a are constants [25]. PNA and luminol doped PNAs revealed intrinsic viscosities as 0.49, 0.59, 0.61, and 0.55, respectively, which showed that PNA had compact structure but doped three had more expanded chains as compared to pure PNA (Table 1). The viscosity and viscosity average molecular weight of PNA-luminol-acidic was observed to be the highest. The increase in the viscosity and molecular weight of the doped forms of PNA could be attributed to doping by luminol. The elemental analysis results also revealed slight variation in the calculated and found values of %C, %N, and %H content.

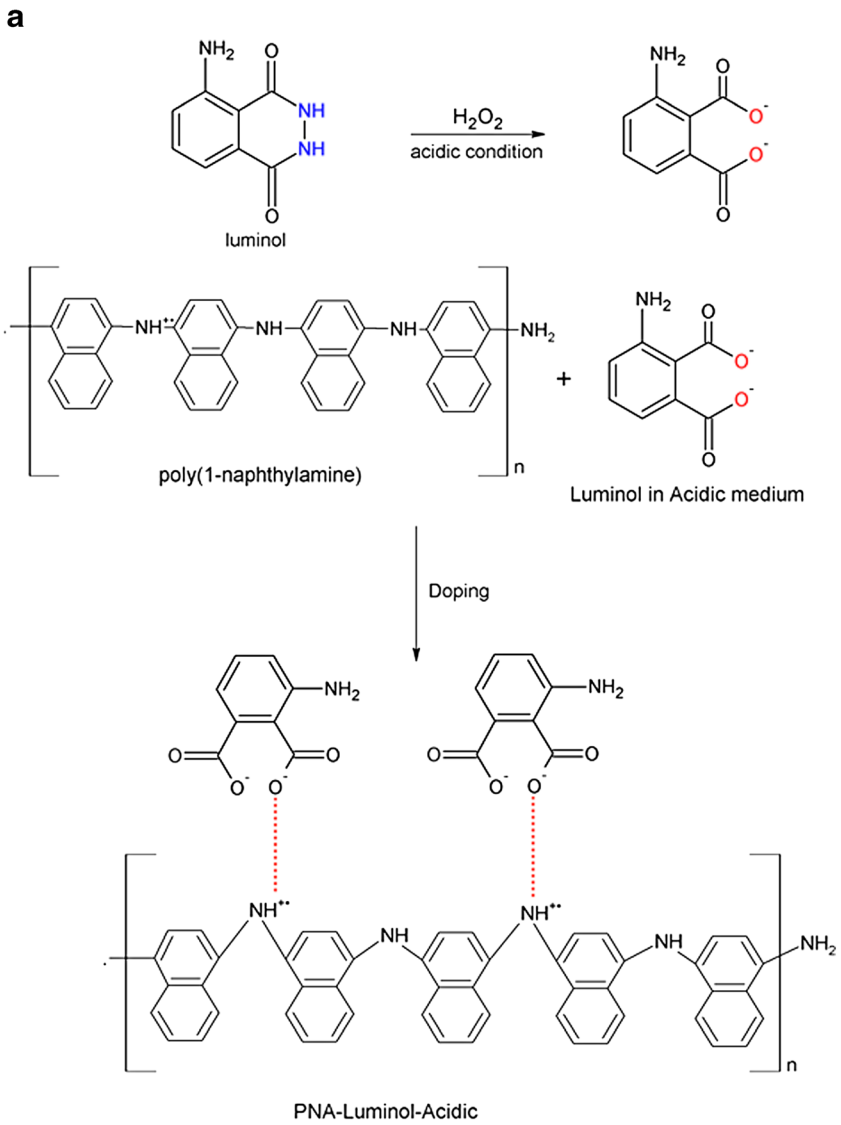

Fig. 1 Proposed structures of doped PNA in **a** acidic, **b** basic, **c** neutral media

The FT-IR spectral data of pure PNA (Table 2) revealed an N–H stretching vibration peak at 3414 cm^{-1}. The NH-imine stretching for PNA appeared at 1639 cm^{-1}, while quinonoid and benzenoid peaks were noticed at 1523 and 1492 cm^{-1}, respectively [28, 29]. The peak corresponding to CN stretching vibration was found at 1253 cm^{-1}, while the band at 765 cm^{-1} was attributed to C-H out-of plane bending vibration. The presence of above peaks confirmed the polymerization of PNA [28, 29]. Upon doping of PNA with luminol in basic medium, the NH stretching peak was observed at 3415 cm^{-1}, while a new peak corresponding to carbonyl oxygen of luminol appeared at 1713 cm^{-1}. The imine stretching peak was noticed to shift to 1620 cm^{-1}, whereas quinonoid and benzenoid peaks were noticed at 1535 and 1490 cm^{-1}, respectively. However, upon doping of PNA with luminol in acidic medium, NH stretching peak was observed at 3421 cm^{-1}, while the C = O stretching peak was noticed at 1690 cm^{-1}. The peaks associated with quinonoid and benzenoid rings appeared at 1513 and 1490 cm^{-1}, respectively. Similar shifting of peaks was noticed when PNA was doped with luminol in neutral medium. The imine stretching peak for PNA-luminol-neutral showed a major shift to 1630 cm^{-1} as compared to pristine PNA, and the absorption intensity was also noticed to be higher as in the case of PNA-luminol-basic. The presence of C = O vibration peak and the variation in absorption intensity of imine stretching peak, quinonoid, and benzenoid peaks confirmed the doping of PNA by luminol. The C-C stretching for the quinonoid peak revealed highest absorption intensity in PNA-luminol-acidic, while the C-C stretching for the benzenoid peak revealed highest absorption intensity in PNA-luminol-basic. The ratio of benzenoid to quinonoid (B/Q) was found to be around 1 for PNA and PNA-luminol-basic, while it was observed to be 0.34 and 0.98, respectively, in PNA-luminol-acidic and PNA-luminol-

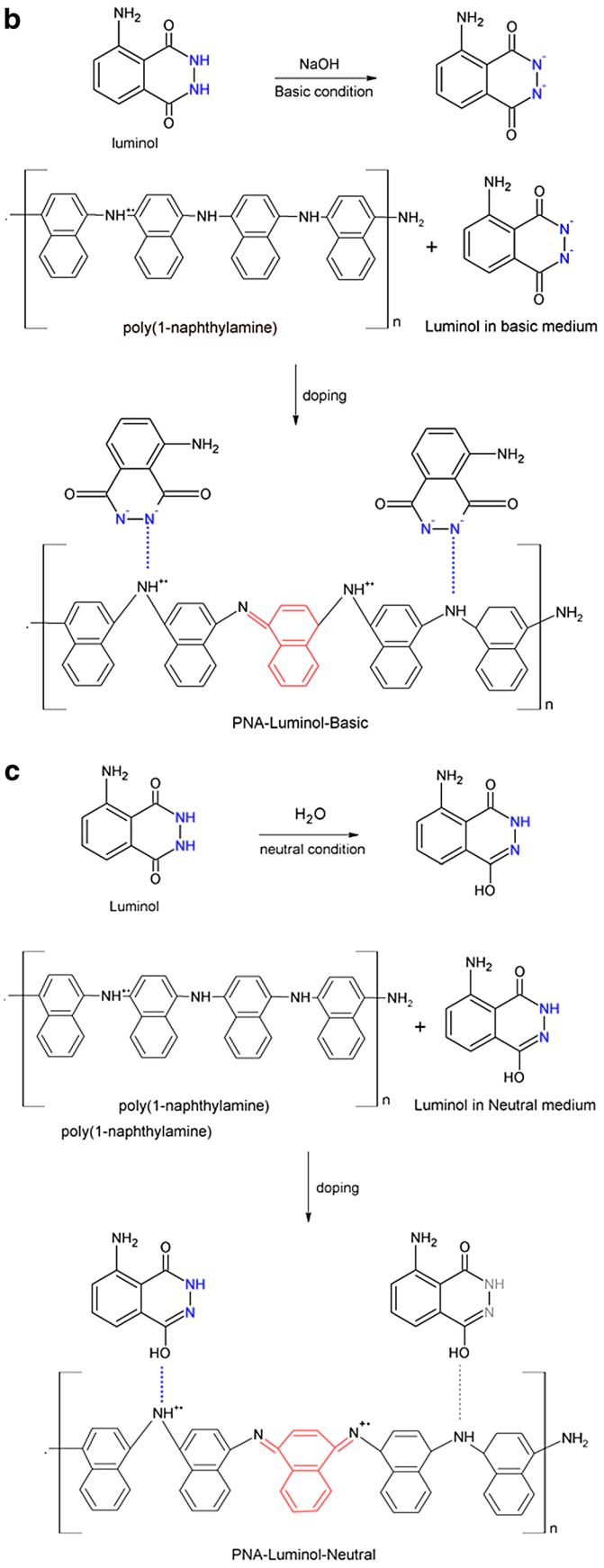

Fig. 1 (continued)

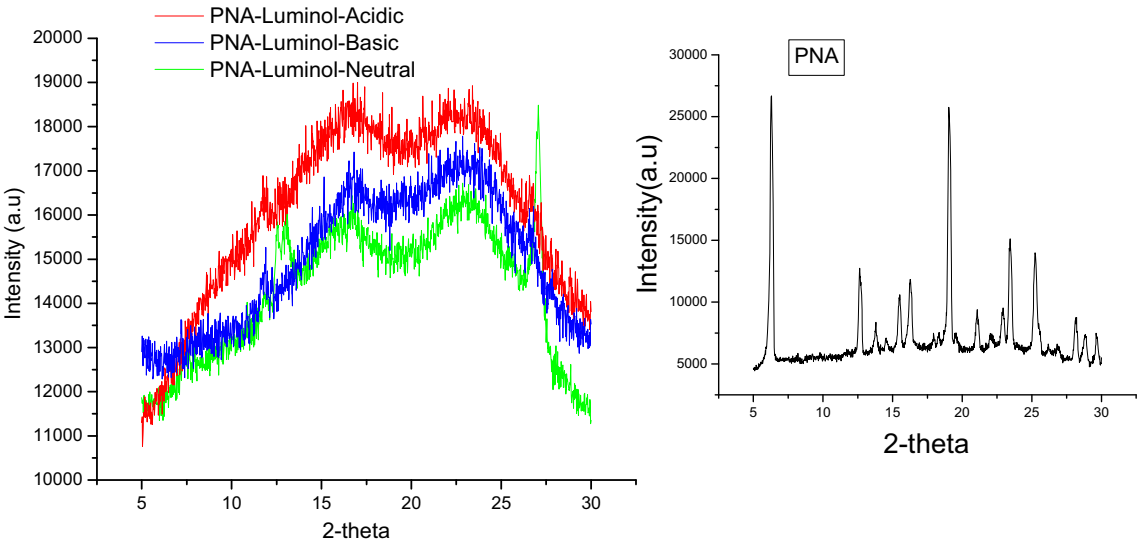

Fig. 2 XRD of PNA (*inset*) and luminol doped PNA

neutral. The lower ratio observed for the later forms indicated that quinonoid form was higher, while in the case of PNA and its doped form in basic solution, higher benzenoid form was noticed [30]. The proposed chemical structure of PNA-luminol-acidic (Fig. 1a) also reveals higher number of benzenoid units which matches well with the FTIR results. In the case of PNA-luminol-basic (Fig. 1b), benzenoid rings are noticed to be in large numbers, while for PNA-luminol-neutral (Fig. 1c), PNA contains quinonoid units in its structure. The nature of bonding is also found to vary with the nature of luminol. For PNA-luminol-acidic and PNA-luminol-neutral, the oxygen of luminol binds electrostatically with the NH of PNA which is also consistent with the variation in the NH stretching peaks in the two cases as seen from the FTIR data. In the case of PNA-luminol-basic, the variation in the NH stretching peak is observed to be insignificant as the structure shows the electrostatic interaction of negatively charged nitrogen on luminol with PNA (Fig. 1b). However, the imine

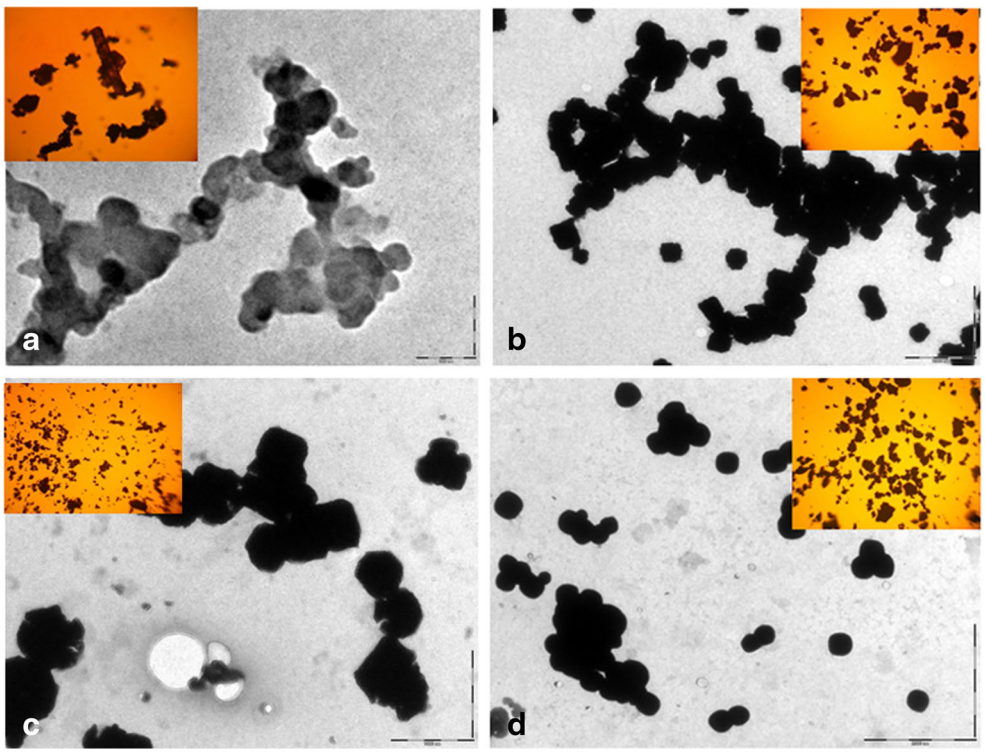

Fig. 3 TEM micrographs of (**a**) PNA, (**b**) PNA-luminol-acidic, (**c**) PNA-luminol-basic, and (**d**) PNA-luminol-neutral

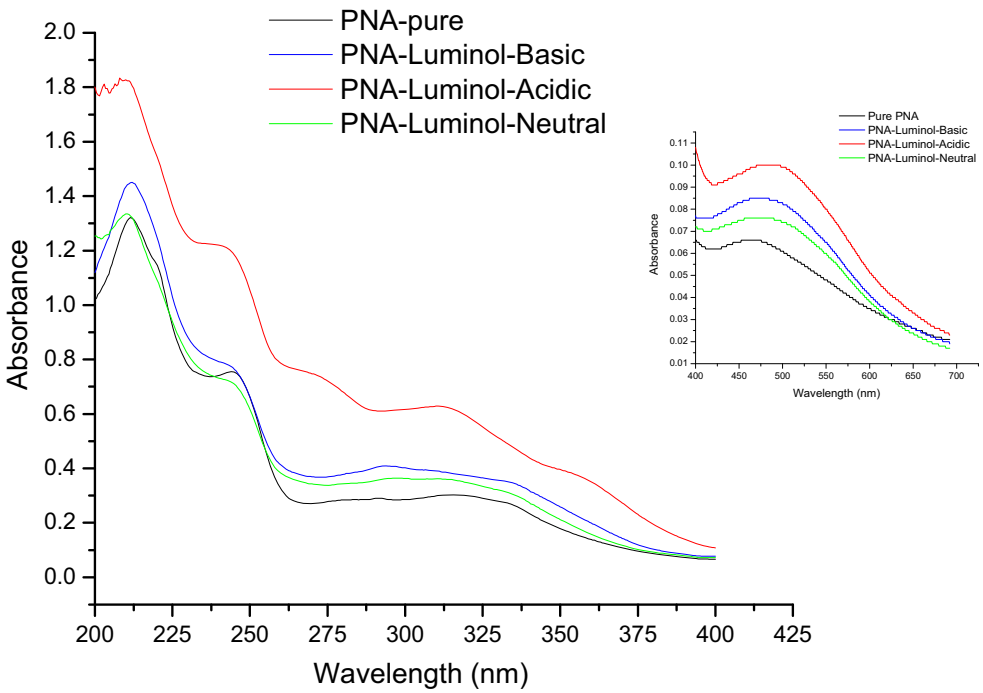

Fig. 4 UV-visible spectra of PNA and luminol doped PNA

stretching peak is seen to be highly shifted (from 1639 to 1620 cm^{-1}) which matches well with the proposed structure.

Morphological studies of PNA and luminol doped PNAs

XRD of pure PNA (Fig. 2) revealed pronounced peaks at 2θ = 6.3°, 12.64°, 16.28°, 19.04°, 23.44°, 25.24°, and 28.22°, suggesting highly crystalline structure of PNA. Upon doping of PNA with different forms of luminol, the highly ordered structure was observed to decline and a semi-crystalline structure was formed which confirmed doping of PNA with luminol [28–30]. The peak intensity of PNA-luminol-neutral was observed to be the lowest, while that of PNA-luminol-acidic was observed to be highest indicating that the structure of the later was partly crystalline and some ordered PNA chains were present. The presence of broad humps revealed intense changes in the crystalline morphology as well as ordering of chains upon doping of PNA with luminol [28–30].

The TEM micrograph of PNA (Fig. 3a) showed fused hollow rod-like structure, while PNA-luminol-acidic (Fig. 3b) revealed fused dense cubic particles forming a chain-like structure. The particles of PNA-luminol-basic (Fig. 3c) revealed dense morphology of spheres and cube-like structures, while PNA-luminol-neutral (Fig. 3d) revealed scattered spherical aggregates. The structure of pristine PNA appeared to be hollow, but upon doping, dense black aggregated morphology was obtained which is consistent with the optical images as well (shown in inset). The optical micrographs were taken at magnification (×1000), and PNA (Fig. 3a, inset) revealed a fibrous morphology. Upon doping with luminol in acidic medium (Fig. 3b, inset), scattered sense particles were observed having distorted spherical structures. The optical micrograph of PNA-luminol-basic (Fig. 3c, inset) and PNA-luminol-neutral (Fig. 3d, inset) revealed clusters of tiny particles joining to form aggregates. The presence of dense morphology confirmed doping of PNA with luminol. The particles were noticed to form a self-assembled network-like structure of having mixed morphology of cubes and spheres.

Table 3 UV data PNA and luminol doped PNA

Sample	λ_{max} (nm)	$\int ad\bar{\nu}$ (integrated absorption coefficient), cm^{-2}	Molar extinction coefficient	Oscillator strength
PNA	500	210.00	2371.54	0.03
PNA-luminol-basic	500	358.00	3057.85	0.06
PNA-luminol-acidic	500	445.25	3607.62	0.07
PNA-luminol-neutral	500	298.16	2740.21	0.05

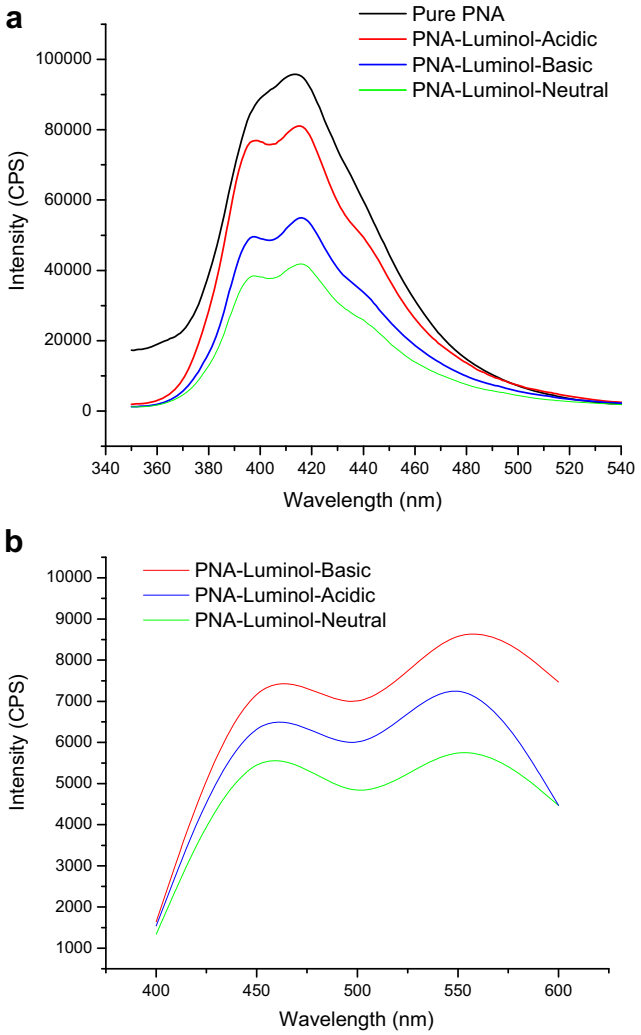

Fig. 5 Fluorescence emission spectra of PNA and luminol doped PNA in **a** solution state and **b** solid state

Optical characteristics of PNA and luminol doped PNA analyzed by UV-visible and fluorescence spectra

The UV–visible spectra of pure PNA and doped PNA were taken in THF and are depicted in Fig. 4. Pure PNA revealed peaks at 210, 245, and 325 nm in the UV range associated with π-π^* transition and 500 nm in the visible range (shown in inset) due to the polaronic transition [28–30]. Upon doping of PNA with luminol, the intensities of the π-π^* transition and polaronic transition were found to vary depending upon state of luminol in the acidic, basic, and neutral media. The intensity of the peaks highly increased upon doping with luminol in acidic medium and basic medium. The oscillator strength, molar extinction coefficient, and integrated absorption coefficient were also found to be in the order PNA-luminol-acidic > PNA-luminol-basic > PNA-luminol-neutral > PNA. Higher values of oscillator strength revealed higher electron transition ability in this polymer, while lower values revealed unfavorable configuration of HOMO and LUMO orbitals because of reduced electron density of benzene ring. The oscillator strength was observed to be 0.03, 0.07, 0.06, and 0.05 for PNA, PNA-luminol-acidic, PNA-luminol-basic, and PNA-luminol-neutral, “”respectively (Table 3). On the basis of the above observations, it can be concluded that doping of PNA with luminol increases the electron transition ability of this polymer as compared to its pristine form which can be tuned to obtain desired optoelectronic properties. Based on the proposed structures for the doped forms of PNA, it can be noticed that the presence of 3-aminophthalate structure on alternate PNA chains in acidic medium is responsible for providing higher polaronic transition intensity (Fig. 1a). The above observations are also corroborated by the fluorescence emission spectra. The emission spectrum of pure PNA and doped PNA in THF is shown in Fig. 5. The fluorescence spectrum of PNA (λ_{exc} = 330 nm) revealed a broad emission peak at 420 nm which was correlated to $S_0 \rightarrow S_1$ transition. Upon doping of PNA with luminol, the emission intensity of PNA was found to decrease revealing quenching of PNA by luminol (Fig. 5a). Splitting of emission peaks was noticed, and two peaks were observed around 380 and 420 nm, respectively. A slight shoulder was also observed around 480 nm. The peak found at 420 nm was related to the emission peak of pristine luminol [18]. This observation confirmed that doping of luminol introduced structural changes in PNA. Among the three doped polymers, PNA-luminol-acidic revealed the highest emission intensity. However, the solid state spectra of PNA and luminol doped PNAs revealed emission intensities around 480 and 550 nm (λ_{exc} = 330 nm), while no such peak was noticed for pristine PNA (Fig. 5b). The emission peak was correlated to $S_0 \rightarrow S_1$ transition. The emission intensity was observed to be maximum for PNA-luminol-acidic as in the case of the spectrum in the solution state. The absence of the peaks at 480 and 550 nm in the solution state is attributed to the solvent

Table 4 Fluorescence data of PNA and doped PNA

Sample	λ_{max} (nm)	A_{sample}	Integrated area	Quantum yield (ϕ)
PNA	419	0.062	7.11×10^6	6×10^{-3}
PNA-luminol-basic	411	0.076	2.97×10^6	4.2×10^{-2}
PNA-luminol-acidic	415	0.093	5.7×10^6	6.7×10^{-2}
PNA-luminol-neutral	414	0.070	3.8×10^6	3.3×10^{-2}

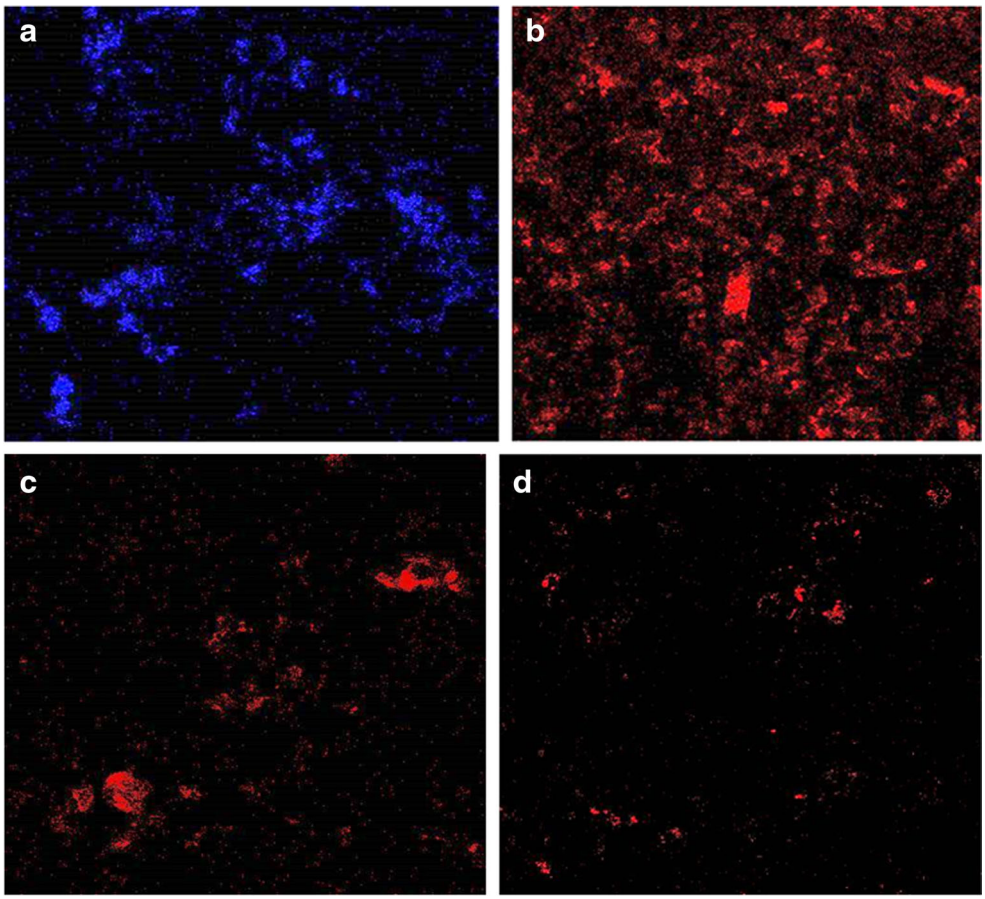

Fig. 6 Confocal micrographs of **a** PNA, **b** PNA-luminol-acidic, **c** PNA-luminol-basic, and **d** PNA-luminol-neutral

effect which causes intense hydrogen bonding. The values of quantum yield (ϕ) were calculated and are given in Table 4. The quantum yield (ϕ) was noticed to be 6×10^{-3} for PNA, while upon doping, these values were 4.2×10^{-2}, 6.7×10^{-2}, and 3.3×10^{-2}, respectively, for PNA-luminol-basic, PNA-luminol-acidic, and PNA-luminol-neutral. Among all the luminol doped forms of PNA, PNA-luminol-acidic revealed highest quantum yield (Table 4). This can be correlated to the oxidation of luminol under highly acidic conditions to produce 3-aminophthalate. The presence of oxygen-rich sites in 3-aminophthalate is presumably responsible for the high quantum yield of PNA in acidic medium.

The confocal micrograph of PNA in solid state (Fig. 6a) exhibited intense blue emission, but upon doping with luminol in acidic medium (Fig. 6b), intense red emission was obtained. The intensity of the red emission was observed to be lower for PNA-luminol-basic (Fig. 6c), as compared to PNA-luminol-acidic. PNA-luminol-neutral (Fig. 6d) also revealed lower emission intensity in the red region. The confocal micrograph of PNA-luminol-acidic (Fig. 6b) revealed a clear dispersion of discrete tiny particles. Upon doping of PNA with luminol in basic medium (Fig. 6c), the particles appeared to be more clustered, while in PNA-luminol-neutral (Fig.6d), the confocal micrograph revealed less aggregation as well as intensity. It can therefore be concluded that intense red emission was observed upon doping of PNA in acidic medium and this polymer could be used for designing NIR agents for live cell imaging.

Conclusion

PNA was successfully synthesized via ultrasonication technique and doped with luminol under acidic basic and neutral conditions. Polymerization and doping was confirmed by FTIR and elemental analysis, while UV studies confirmed structural variations. XRD revealed crystalline morphology of PNA, while the doped forms were found to be semicrystalline. Fluorescence studies confirmed that highest quantum yield was attained in the case of PNA doped in acidic medium and its confocal micrographs revealed intense red emission. The results showed that doping of PNA with various forms of luminol attained in acidic, basic, and neutral medium could be utilized to design polymers for imaging of biological analytes by optimizing the doping conditions.

Acknowledgements The corresponding author Dr. Ufana Riaz wishes to acknowledge the DST-SERB for granting major research project-wide sanction number SB/S1/PC-070/2013. The coauthor Mrs. Sapana Jadoun is thankful to DST-SERB for granting Junior Research Fellowship under the said project. The authors also acknowledge the SAIF Facility at All India Institute of Medical Sciences (AIIMS), New Delhi, India, for TEM analysis and the Advance Instrumentation Research Facility (AIRF) at JNU, Delhi, India, for the Confocal Analysis.

Compliance with ethical standards

Conflict of interest The authors declare that they have no conflict of interest.

References

1. Lesiak B, Kosinski A, Krawczyk M, Zommer L, Jablonski A (2000) Characterization of polyacetylene and polyacetylene doped with palladium, polish. J Chem 865:847–865
2. Liu Z, Zhu Y, Wang L, Ding C (2011) Polyaniline Microtubes with a hexagonal cross-section and pH-sensitive fluorescence properties. MacromolRapidCommun 32:512–517
3. De Melo EF, Alves KGB (2013) Synthesis of fluorescent PVA / polypyrrole-ZnO nanofibers. JMaterSci 48:3652–3658. doi:10.1007/s10853-013-7159-2
4. Barbara S (1996) Efficient photoluminescence and electroluminescence from a soluble Polyfluorene. JAmChemSoc 118:7416–7417
5. Wu P, Kim FS, Jenekhe SA (2011) New poly (arylene vinylene) s based on Diketopyrrolopyrrole for Ambipolar transistors. ChemMater 23:4618–4624
6. Liu H, Espe M, Modarelli DA, Arias E, Moggio I, Ziolo RF, Heinz H (2014) Interaction of substituted poly(phenyleneethynylene)s with ligand-stabilized CdS nanoparticles. MaterChem A 2:8705–8711
7. Adenier CLA, Chane-Ching KI, Maurel F (2006) A novel fluorescent , conducting polymer: electrosynthesis , characterization and optical properties. SynthMet 156:256–269
8. Riaz U, Ashraf SM (2011) Semi-conducting poly(1-naphthylamine) nanotubes: a pH independent adsorbent of sulphonate dyes. Chem Eng J 174(2–3):546–555
9. Riaz U, Ashraf SM, Kumar S, Ahmad I (2014) Controlling the growth of polycarbazole within the silicate galleries using peroxides via microwave-assisted green synthesis. Chem Eng J 241:259–267
10. Balint R, Cassidy NJ, Cartmell SH (2014) Conductive polymers: towards a smart biomaterial for tissue engineering. ActaBiomater 10:2341–2353
11. A. Milica M. Gvozdenović, B.Z. Jugović, J.S. Stevanović, T.L. Trišović and B.N. Grgur, Electrochemical Polymerization of Aniline, Electropolymerization, (2011). Ewa Schab-Balcerzak (Ed.), ISBN: 978–953–307-693-5, InTechopen
12. Riaz U, Ahmad S, Ashraf SM (2008) Template free synthesis of nanoparticles of poly (1-naphthylamine): influence of alcoholic medium on polymerization. ColloidPolymSci 286(4):459–462
13. Riaz U, Ashraf SM, Farooq M (2015) Effect of pH on the microwave-assisted degradation of methyl orange using poly(1-naphthylamine) nanotubes in the absence of UV–visible radiation. Colloid.Polym.Sci. 293(4):1035–1042
14. Riaz U, Ahmad S, Ashraf SM (2008) Influence of polymerization conditions on the template free synthesis of nanoparticles of poly (1-naphthylamine). PolymBull 60(4):487–493
15. Shu J, Wang W, Cui H (2015) Direct electrochemiluminescence of gold nanoparticles bifunctionalized by luminol analogue–metal complexes in neutral and alkaline media. Chem Commun 51: 11366–11369
16. Knight AW (1999) A review of recent trends in analytical applications of electrogenerated chemiluminescence. Trend AnalChem 18: 47–62
17. Chang YT, Lin KC, Chen SM (2005) Preparation, characterization and electrocatalytic properties of poly(luminol) and polyoxometalate hybrid film modified electrodes. Electrochim Acta 51:450–461
18. Barni F, Lewis SW, Berti A, Miskelly GM, Lago G (2007) Forensic application of the luminol reaction as a presumptive test for latent blood detection. Talanta 72:896–913
19. Liu M, Lin Z, Lin J (2010) Analytica Chimica Acta a review on applications of chemiluminescence detection in food analysis. Anal Chim Acta 670:1–10
20. Dodeigne C, Thunus L, Lejeune R (2000) Chemiluminescence as diagnostic tool. A review 51:415–439
21. Proescher F, Moody AM (1939) Detection of blood by means of chemiluminescence. J LabClin Med 24:1183–1118
22. Suslick KS, Price GJ (1999) Applications of ultrasound to materials chemistry. AnnRevMaterSci 29:295–326
23. Noltingk BE, Neppiras EA Cavitation produced by ultrasonics. Proceedings of the Physical Society Section B 63:674–685
24. Wu YJ, Ho KS, Cheng YW, Chao L, Wang YZ, Hsieh TH, Ho TH, Han YK (2013) Studies on the synthesis of low molecular weight, one-dimensional polyanilines prepared by fast emulsion polymerization using (n-dodecylbenzenesulfonic acid)/HCl emulsifiers. Polym Int 62:581–590
25. Garai A, Chatterjee S, Nandi AK (2010) Nanocomposites of silver nanoparticle and Dinonylnaphthalene Disulfonic acid-doped Thermoreversible Polyaniline. GelPolymEngSci 50:446–454
26. Riaz U, Ashraf SM, Aleem S, Budhiraja V, Jadoun S (2016) Microwave-assisted green synthesis of some nanoconjugated copolymers: characterisation and fluorescence quenching studies with bovine serum albumin. New J Chem 40:4643–4653
27. Riaz U, Ashraf SM (2012) Microwave-assisted solid state in situ polymerization and intercalation of poly (carbazole) between Bentonite layers: effect of microwave irradiation and gallery. J Phys Chem C 116:12366–12374
28. Riaz U, Ahmad S, Ashraf SM (2008) Pseudo template synthesis of poly (1-naphthylamine): effect of environment on nanostructured morphology. J Nanopart Res 10:1209–1214
29. Riaz U, Jahan R, Ahmad S, Ashraf SM (2008) Copolymerization of poly(1-naphthylamine) with aniline and o-toluidine. J Appl Polym Sci 108:2604–2610
30. Riaz U, Ashraf SM, Ruhela A (2015) Catalytic degradation of orange G under microwave irradiation with a novel nanohybrid catalyst. JEnvChemEngg 3(1):20–29